JOURNAL OF THEORETICAL
AND APPLIED MECHANICS
1, 36, 1998

MODELLING AND ANALYSIS OF SHELL CASE DYNAMICS

JERZY MANEROWSKI

MIROSŁAW NOWAKOWSKI

Air Force Institute of Technology, Warsaw

The paper deals with physical, mathematical and computer models of dynamics of a shell case. The model has been formulated using the results of studying the dynamics of flying objects as well as data obtained from wind tunnel tests. A numerical method of integrating the Runge-Kutta-Gill equations has been used to solve a system of ordinary differential equations that describe the shell case motion
The model has been applied to:
– Analysis of parameters of motion of the aircraft gun shell case dropped from the aircraft in any 3D motion, with real parameters of the atmosphere and the air mass motion (wind and airflow behind the wing) taken into account;
– Determination of zones of dispersion of shell cases in space and relative to the second-in-the-pair airplane while attacking targets in the course of formation flying.

Key words: aircraft gun shell, model of dynamics of a shell case, zone of dispersion of a shell case

1. Introduction

What has been given consideration throughout the paper is dynamics of a shell case ejected from an aircraft gun.

The question of constructing a model that enables parameters of motion of a shell case (dropped from an airplane in any three-dimensional flight) to be determined has resulted from specific needs of aircraft designers and operators and falls within the range of flying safety issues.

The work has been effected directly by air accidents. By way of example, a collision of a second-in-the-pair fighter with shell cases ejected from a gun of a lead fighter took place while firing guns in the course of pair operation. The engine and some structural components of the fuselage of the second fighter were damaged then.

Analysis of motion as well as determination of zones of dispersion of shell cases from the aircraft gun, with physical, mathematical and computer models applied, are the primary objectives of the paper.

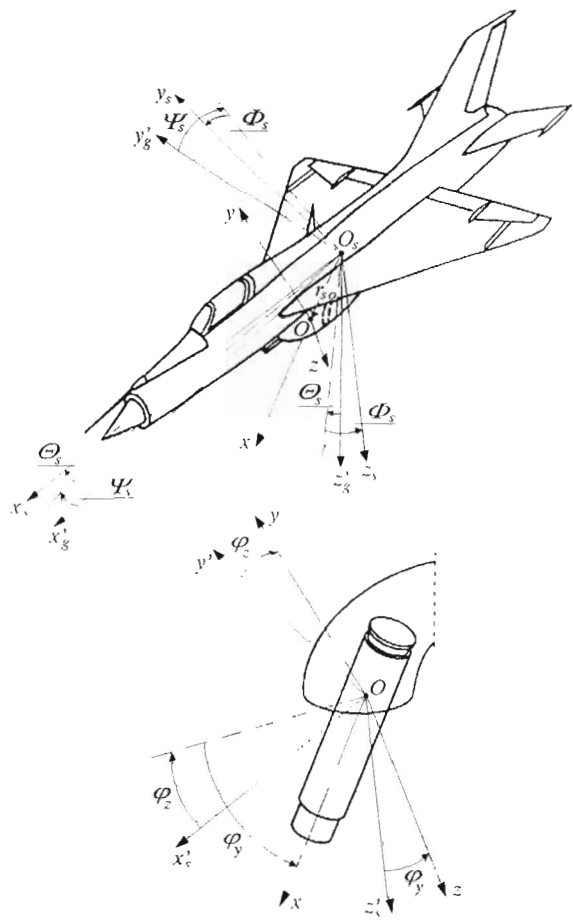

Fig. 1 Co-ordinate systems

Therefore, motion of shell case ejected from the gun of the lead aircraft via its shell-case ejection system has been given consideration. Zones of dispersion of shell cases in space and relative to the second-in-the-pair airplane have been determined as well (Fig.1).

2. Model of shell case motion

It has been assumed in the paper that the shell case travels through the real atmosphere and the air mass moves relative to the ground (cf Manerowski, 1990). Therefore, the resultant vectors of linear velocity $\boldsymbol{V}_c$ and angular velocity $\boldsymbol{\Omega}_c$ of the shell case relative to the ground are the geometrical sums of the shell case velocities relative to the travelling air mass $\boldsymbol{V}_{co}$, $\boldsymbol{\Omega}_{co}$ and of velocities of the air mass relative to the ground $\boldsymbol{V}_{cws}$, $\boldsymbol{\Omega}_{cws}$ (Fig.2)

$$\begin{aligned} \boldsymbol{V}_c &= \boldsymbol{V}_{co} + \boldsymbol{V}_{cws} \\ \boldsymbol{\Omega}_c &= \boldsymbol{\Omega}_{co} + \boldsymbol{\Omega}_{cws} \end{aligned} \tag{2.1}$$

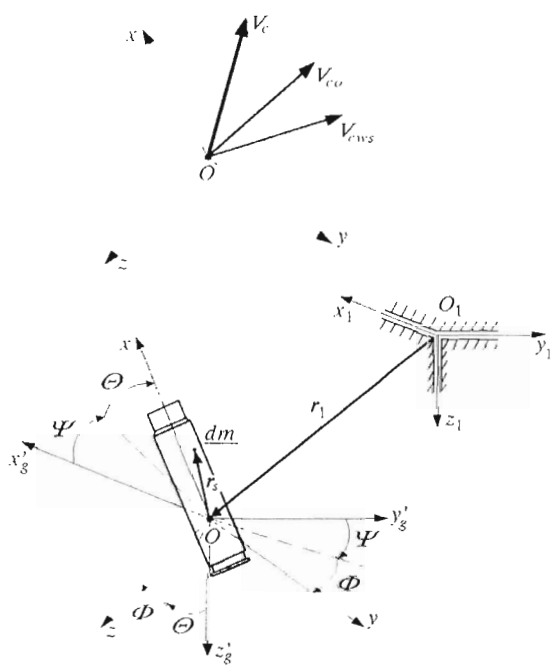

Fig. 2. Vectors of linear velocity of a shell case with the air mass taken into account

Next, the vectors $\boldsymbol{V}_{cws}$, $\boldsymbol{\Omega}_{cws}$ are geometrical sums of velocities of the air mass travelling relative to the ground, i.e. $\boldsymbol{V}_{cw}$, $\boldsymbol{\Omega}_{cw}$, and velocities of the airflow behind the wing shifting relative to the aircraft, i.e. $\boldsymbol{V}_{cs}$, $\boldsymbol{\Omega}_{cs}$

$$\boldsymbol{V}_{cws} = \boldsymbol{V}_{cw} + \boldsymbol{V}_{cs}$$
$$\boldsymbol{\Omega}_{cws} = \boldsymbol{\Omega}_{cw} + \boldsymbol{\Omega}_{cs} \tag{2.2}$$

The absolute acceleration of the elementary mass of the shell case dm has been determined first in order to determine the forces and moments of forces of inertia. Applying fundamental laws of dynamics (cf Susłow, 1960), the absolute acceleration of mass dm (Fig.2) is a sum of relative acceleration $\boldsymbol{a}_{dmw}$ convection $\boldsymbol{a}_{dmu}$ and the Coriolis accoleration $\boldsymbol{a}_{dmC}$, respectively. We can, therefore, write

$$\begin{aligned}
&\boldsymbol{a}_{dm} = \boldsymbol{a}_{dmw} + \boldsymbol{a}_{dmu} + \boldsymbol{a}_{dmC} \\
&\boldsymbol{a}_{dmw} = \dot{\boldsymbol{V}}_{co} + \boldsymbol{\Omega}_{co} \times \boldsymbol{V}_{co} + \boldsymbol{\Omega}_{co} \times (\boldsymbol{\Omega}_{co} \times \boldsymbol{r}_s) + \dot{\boldsymbol{\Omega}}_{co} \times \boldsymbol{r}_s \\
&\boldsymbol{a}_{dmu} = \dot{\boldsymbol{V}}_{cws} + \boldsymbol{\Omega}_{cws} \times \boldsymbol{V}_{cws} + \boldsymbol{\Omega}_{cws} \times (\boldsymbol{\Omega}_{cws} \times \boldsymbol{r}_s) + \dot{\boldsymbol{\Omega}}_{cws} \times \boldsymbol{r}_s \\
&\boldsymbol{a}_{dmC} = 2\boldsymbol{\Omega}_{cws} \times (\boldsymbol{V}_{co} + \boldsymbol{\Omega}_{co} \times \boldsymbol{r}_s)
\end{aligned} \tag{2.3}$$

Below, there are dependences that determine the forces and moments of forces acting upon the shell case in any 3D motion.

Vectors of forces of inertia $\boldsymbol{B}$ and of moments of forces of inertia $\boldsymbol{M}_B$ to which the shell case is subject are given as follows

$$\boldsymbol{B} = \int_{V_m} \boldsymbol{a}_{dm}\, dm$$
$$\boldsymbol{M}_B = \int_{V_m} \boldsymbol{r}_s \times \boldsymbol{a}_{dm}\, dm \tag{2.4}$$

The results of wind tunnel tests for the angles of attack α ranging from 0 to 2π have been applied to determination of aerodynamic forces and moments. Fig.3 shows the results, i.e. the drag coefficient C_{Da}, lift coefficient C_{La}, and coefficient of the pitching moment C_{moya} versus the angle of attack (cf Maryniak and Nowakowski, 1990).

Some fundamental relations of analytic geometry have been used to present the velocity vector $\boldsymbol{V}_{co}$ in the $Oxyz$ frame of reference in the following form

$$\boldsymbol{V}_{co} = |\boldsymbol{V}_{co}| \begin{bmatrix} \cos\alpha \\ \cos\gamma \\ \cos\eta \end{bmatrix} \tag{2.5}$$

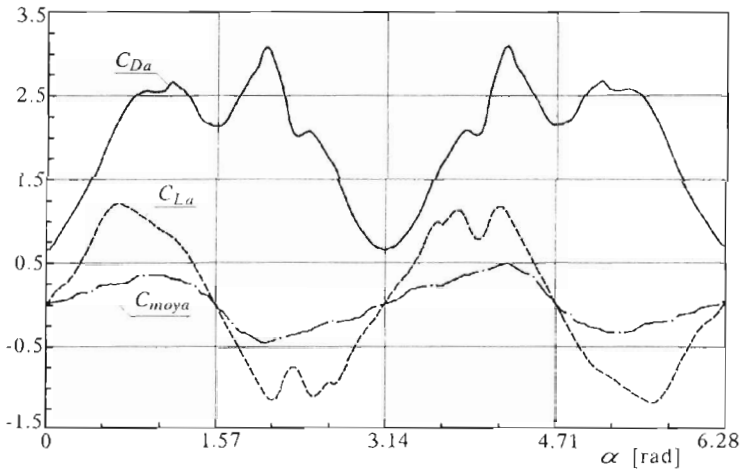

Fig. 3. Aerodynamic coefficients

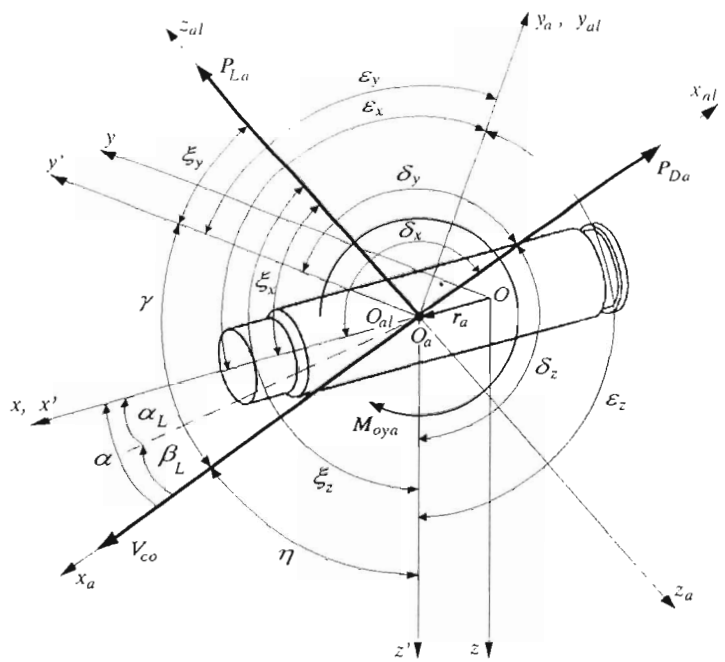

Fig. 4. Angles between the directions of aerodynamic forces in the analytical airflow system $O_{al}x_{al}y_{al}z_{al}$ and in the shell-case-fixed frame of reference $Oxyz$

where

$|V_{co}|$ - absolute value of the linear velocity of a shell case

α, γ, η - angles between the vector V_{co} and the axes of given as follows the shell-case-fixed co-ordinate system (Fig.4)

$$\alpha = \arccos\frac{U_o}{|V_{co}|} \qquad \gamma = \arccos\frac{V_o}{|V_{co}|} \qquad \eta = \arccos\frac{W_o}{|V_{co}|} \tag{2.6}$$

In a similar way the other quantities have been determined, i.e.

- Angles between the direction of aerodynamic lift $\boldsymbol{P}_{La}$ in the analytical airflow system $O_{al}x_{al}y_{al}z_{al}$ and the axes of the shell-case-fixed frame of reference $Oxyz$ (Fig.4)

$$\begin{aligned}
\xi_x &= \arccos\frac{-V_o^2 - W_o^2}{\sqrt{(-V_o^2 + W_o^2)^2 + U_o^2(V_o^2 + W_o^2)}} \\
\xi_y &= \arccos\frac{U_o V_o}{\sqrt{(-V_o^2 + W_o^2)^2 + U_o^2(V_o^2 + W_o^2)}} \\
\xi_z &= \arccos\frac{U_o W_o}{\sqrt{(-V_o^2 + W_o^2)^2 + U_o^2(V_o^2 + W_o^2)}}
\end{aligned} \tag{2.7}$$

- Angles between the direction of axis y_{al} being the axis of pitching moment $\boldsymbol{M}_{oya}$ in the analytical airflow system $O_{al}x_{al}y_{al}z_{al}$ and the axes of the shell-case-fixed frame of reference $Oxyz$ (Fig.4)

$$\varepsilon_x = \frac{\pi}{2} \qquad \varepsilon_y = \arccos\frac{W_o}{\sqrt{V_o^2 + W_o^2}} \qquad \varepsilon_z = \arccos\frac{V_o}{\sqrt{V_o^2 + W_o^2}} \tag{2.8}$$

- Angles between the direction of lift $\boldsymbol{P}_{Da}$ in the analytical airflow system $O_{al}x_{al}y_{al}z_{al}$ and the axes of the shell-case-fixed frame of reference $Oxyz$ (Fig.4)

$$\begin{aligned}
\delta_x &= \arccos\left(-\frac{U_o}{|V_{co}|}\right) \qquad \delta_y = \arccos\left(-\frac{V_o}{|V_{co}|}\right) \\
\delta_z &= \arccos\left(-\frac{W_o}{|V_{co}|}\right)
\end{aligned} \tag{2.9}$$

Equations of any 3D shell case motion (cf Manerowski, 1990) under the assumptions about the air mass motion (i.e. wind and airflow behind the

wing) accepted have in the following form

$$\dot{V}_{\Omega o} = -\dot{V}_{\Omega ws} - \mathbf{B}_m^{-1}\hat{\mathbf{V}}_{\Omega o}\mathbf{B}_m V_{\Omega o} - \mathbf{B}_m^{-1}\hat{\mathbf{V}}_{\Omega ws}\mathbf{B}_m V_{\Omega ws} + \mathbf{B}_m^{-1}(F_G + F_A - F_C) \tag{2.10}$$

where

- $\mathbf{B}_m$ – matrix of inertia
- $\hat{\mathbf{V}}_{\Omega o}$ – matrix of linear and angular velocities of the shell case relative to the air
- $\hat{\mathbf{V}}_{\Omega ws}$ – matrix of linear and angular velocities of the air mass
- $V_{\Omega o}$ – vector of linear and angular velocities of the shell case relative to the air mass in motion
- $V_{\Omega ws}$ – vector of linear and angular velocities of the air mass
- F_A, F_C, F_G – vectors of aerodynamic forces and of moments of aerodynamic forces, forces of inertia and gravity.

The following relations have been used to describe the shell case motion in space:

— kinematic relations of linear velocity

$$\dot{X} = \mathbf{E}^{\top}(V_{co} + V_{cws}) \tag{2.11}$$

– kinematic relations of angular velocity

$$\dot{\Phi}_E = \mathbf{E}_{\Omega}^{\top}(\Omega_{co} + \Omega_{cws}) \tag{2.12}$$

where

- $\dot{X}$ – vector of generalized velocities, $\dot{X} = [\dot{x}_1, \dot{y}_1, \dot{z}_1]^{\top}$
- $\dot{\Phi}_E$ – vector of angular velocities, $\dot{\Phi}_E = [\dot{\Phi}, \dot{\Theta}, \dot{\Psi}]^{\top}$
- $\mathbf{E}$ – orthonormal matrix of the Euler angles

$$\mathbf{E} = \begin{bmatrix} \cos\Psi\cos\Theta & \sin\Psi\cos\Theta & -\sin\Theta \\ \cos\Psi\sin\Theta\sin\Phi + & \sin\Psi\sin\Theta\sin\Phi + & \cos\Theta\sin\Phi \\ -\sin\Psi\cos\Theta & -\cos\Psi\cos\Theta & \\ \cos\Psi\sin\Theta\cos\Phi + & \sin\Psi\sin\Theta\sin\Phi + & \cos\Theta\cos\Phi \\ +\sin\Psi\sin\Phi & -\cos\Psi\sin\Phi & \end{bmatrix}$$

- $\mathbf{E}_{\Omega}$ – matrix of transformation

$$\mathsf{E}_{\Omega} = \begin{bmatrix} 1 & 0 & -\sin\Theta \\ 0 & \cos\Phi & \sin\Phi\cos\Theta \\ 0 & -\sin\Theta & \cos\Phi\cos\Theta \end{bmatrix}$$

3. Numerical analysis

With the mathematical/physical/computer model (Manerowski et al., 1990) formulated the primary parameters of the shell case motion have been determined under the following conditions:

- Atmosphere at rest – the components of the air mass velocity, i.e. of wind and airflow behind the wing equal zero
- Air mass in motion – non-zero components of the velocity have been determined at the nodes of an element of space.

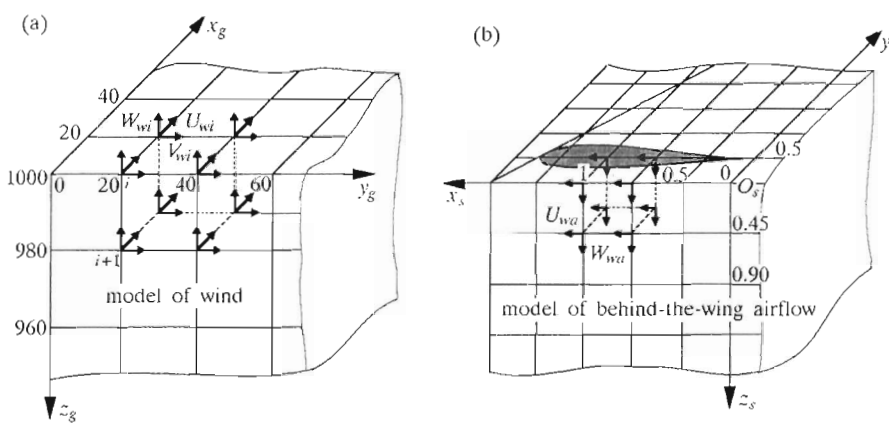

Fig. 5. Models of the wind and behind-the-wing airflow

Distances between the nodes are:

(a) wind models I and II: 20 m (Fig.5a),

(b) model of airflow behind the wing (Fig.5b): in plane $O_s x_s y_s$ – 0.5 m, in plane $O_s x_s y_s$ – 0.45 m.

The calculations were made assuming a linear change of velocity within the element of space.

In the case of wind model I (Fig.5a) the components in the ith node have been presented in the form: $U_{wi} = 0\,\mathrm{m/s}$, $V_{wi} = 15\,\mathrm{m/s}$, and modulus of vertical velocity $W_{wi} = 5\,\mathrm{m/s}$. It should be noted that the vertical component sho ws reversal of sign in subsequent nodes: in the node i $W_{wi} = 5\,\mathrm{m/s}$, whereas in the node $i+1$ $W_{wi+1} = -5\,\mathrm{m/s}$, etc.

In the case of wind model II (Fig.5a) the components have been determined in the same way, but with the modulus of vertical velovity $W_{wi} = 10\,\mathrm{m/s}$.

In the model of the airflow behind the wing (Fig.5b) distribution of velocities along the wing chord has been described for velocity $V_{os} = 100\,\mathrm{m/s}$.

Computations have been made for the following initial conditions:

- airspeed $V_{os} = 100\,\mathrm{m/s}$
- aicraft flight altitude $h = 1000\,\mathrm{m}$
- angle of pitch $\Theta_s = 0\,\mathrm{rad}$
- velocity of shell case ejection from the aircraft gun $V_{ol} = 21\,\mathrm{m/s}$
- angle of pitch of the shell case on the outlet of the shell-case ejection system $\varphi_y = -1.309\,\mathrm{rad}$
- angle of yaw of the shell case on the outlet of the shell-case ejection system $\varphi_z = 0.227\,\mathrm{rad}$

Fig.6 and Fig.7 show the shell-case flight paths $z_1 = z_1(x_1)$ and $x_1 = x_1(y_1)$. Taking wind into account significantly affects the shell-case flight path. As vertical velocity of wind V_{wi} increases, the shell-case flight path becomes more and more flat (Fig.6a). The shell-case flight paths with both the behind-the-wing airflow and wind taken into account are steeper (Fig.6b) than the flight paths with only models of wind (Fig.6a) given consideration. The same conclusions can be drawn from the shell-case flight paths in the plane $x_1 y_1$ (Fig.7).

Fig.8 illustrates the changes in the shell case velocities versus $V_c = V_c(t)$ with and without giving consideration to the air mass motion. In both the instances the shell case velocities (with models of wind only taken into account) do not differ significantly. However, if both the behind-the-wing airflow and the wind are included into analysis of the shell case velocity, the situation becomes substantially different (Fig.8). The shell case stays in the be hind-the-wing airflow for no longer than 0.02 s; in results velocity decreases by 20 per cent.

Angular speed of pitching Q_o and yawing R_o versus time have been presented in Fig.9 and Fig.10. Wind influences these rates to only a slight degree. If the above-shown wind models are taken into account, slight extension of period of oscillation as well as decrease in the amplitudes of angular velocities can

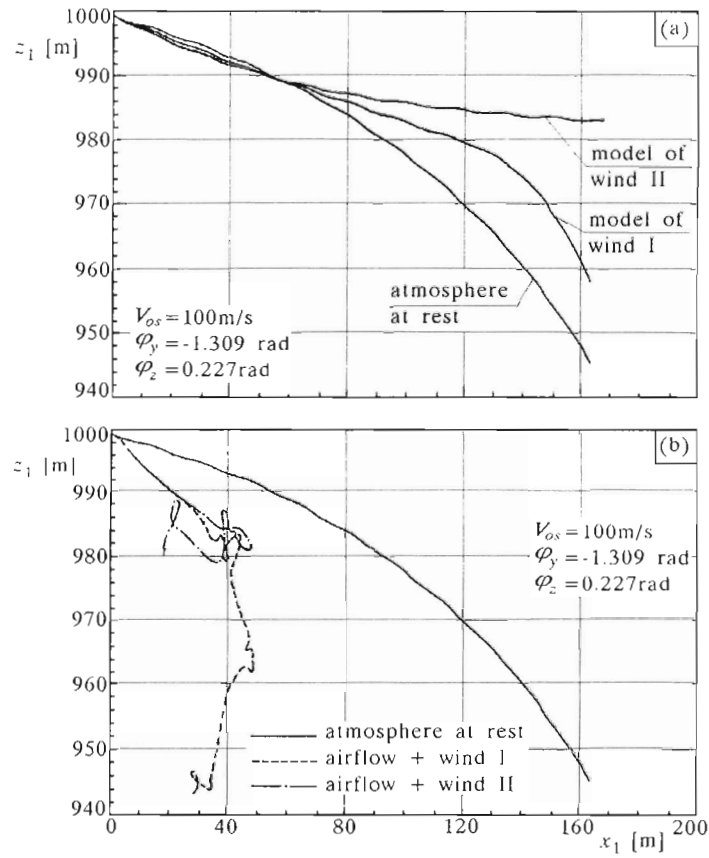

Fig. 6. Flight paths of the shell case $z_1 = z_1(x_1)$ with the air mass motion, i.e. with (a) models of wind, (b) model of the behind-the-wing airflow + wind taken into account

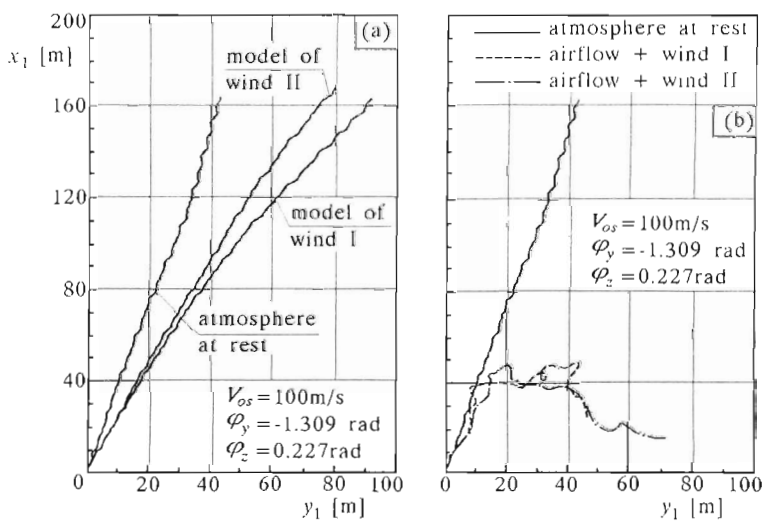

Fig. 7. Flight paths of the shell case $x_1 = x_1(y_1)$ with the air mass motion, i.e. with. (a) models of wind, (b) model of the behind-the-wing airflow + wind taken into account

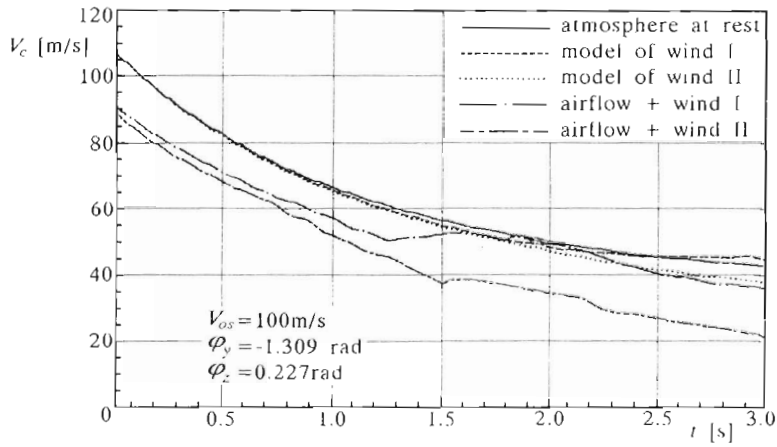

Fig. 8. The shell-case velocities $|V_c|$ versus time with the air mass motion taken into consideration

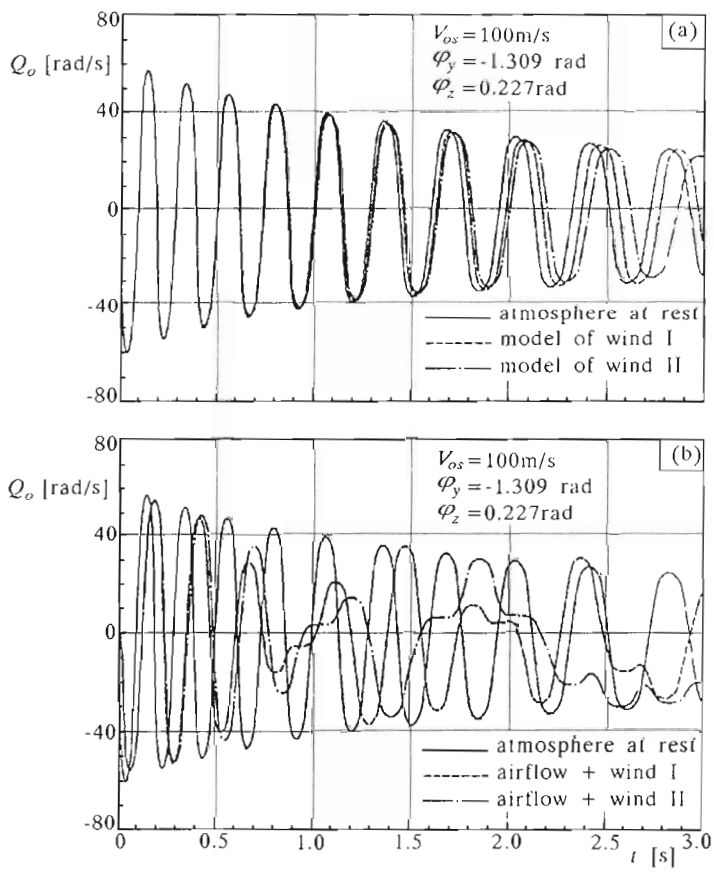

Fig. 9. Angular velocity of pitching of the shell case Q_o versus time with the air mass motion, i.e. with: (a) models of wind, (b) model of the behind-the-wing airflow + wind taken into account

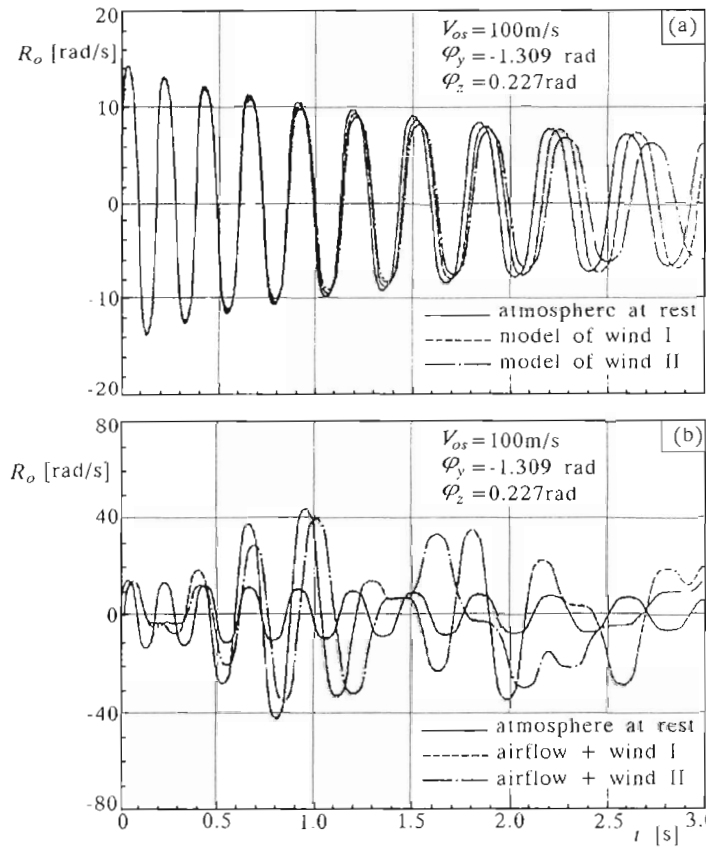

Fig. 10. Angular velocity of yawing of the shell case R_o versus time with the air mass motion, i.e. with. (a) models of wind, (b) model of the behind-the-wing airflow + wind taken into account

be observed. The nature of changes in angular rates of pitching and yawing implies the shell case motion to be the oscillatory, damped motion. Angular velocities of the shell case in the behind-the-wing airflow and in the models of wind (Fig.9b, Fig.10b) show different nature. The shell case motion is not periodic in this instance; damping of motion is evident.

The formulated model has been used to determine potential collisions of the shell case ejected from a lead airplane with other airplanes while attacking targets in the course of formation flying.

The attack was performed by a pair of diving airplanes (at the airplane pitching angle of $\Theta_s = -0.349$ rad) with the following location in space (Fig.11):
- distance between the airplanes measured in the direction of axis x_s – 30 m,

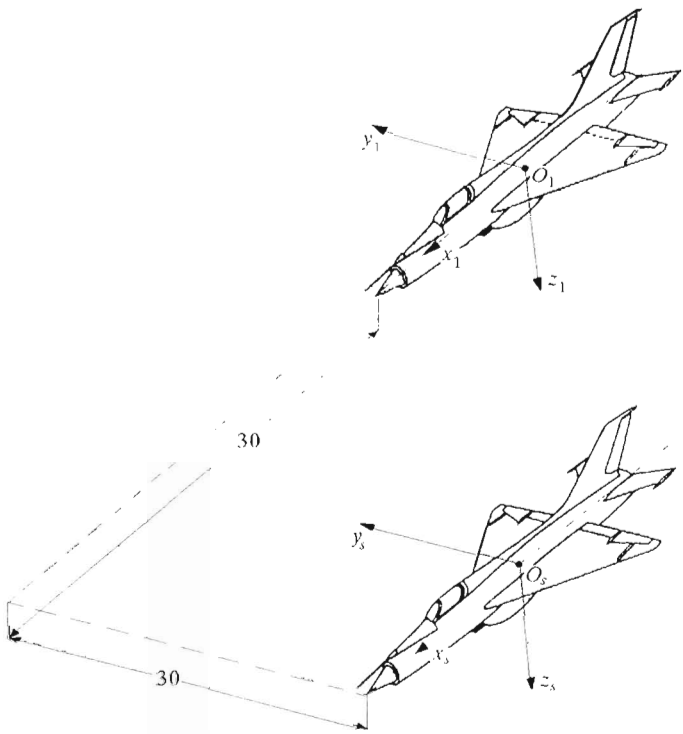

Fig. 11 Location of the aircraft in space

– distance between the airplanes measured in the direction of axis y_s – 30 m,
– gain/loss in height between two airplanes – 0 m.

Computations have been made an the assumption that the angles at which the shell case is ejected relative to the airplane change in vertical plane of the shell-case ejection system: φ_y from -1.239 rad to -1.501 rad, and in horizontal plane of the shell-case ejection system: φ_z from 0.052 rad to 0.401 rad.

The zones of dispersion of shell cases in space have been determined for the shell case in the atmosphere at rest, with the air mass motion taken into account.

Fig.12 shows the co-ordinates of shell case position in the plane perpendicular to the second-in-the-pair airplane (for two airspeeds $V_{os} = 100$ m/s and $V_{os} = 200$ m/s. The points marked in Fig.12 are the co-ordinates of the point of penetration of the above-mentioned plane by the shell case ejected from the lead airplane.

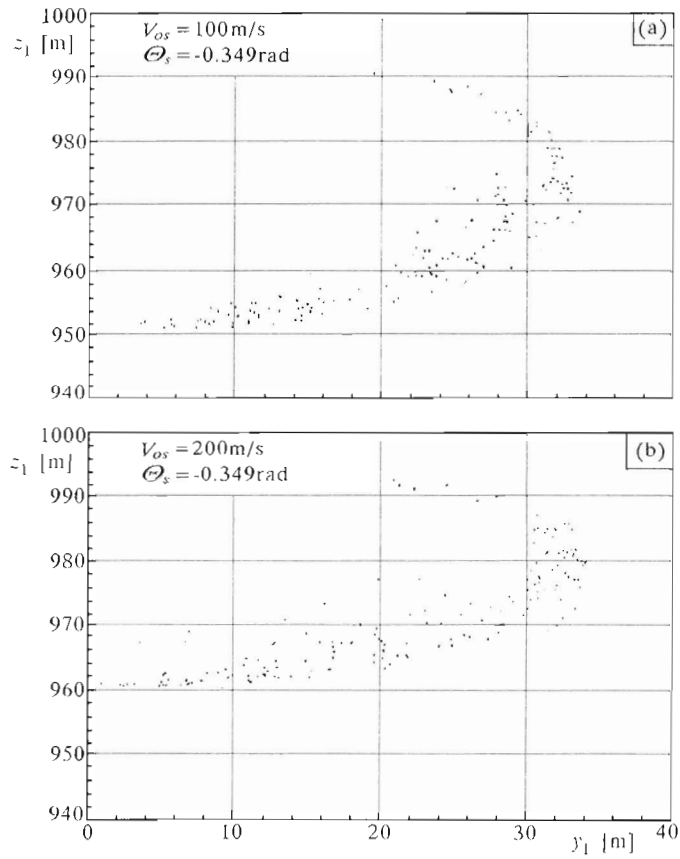

Fig. 12. Zones of dispersion of shell cases in space for aircraft airspeeds: (a) $V_{os} = 100$ m/s, (b) $V_{os} = 200$ m/s

Making computations with regard paid to changes in the initial conditions (i.e. variations of the angle at which the shell case is ejected) a zone of penetration of this plane (points marked with dots) has been determined.

On the basis of the determined zones of penetration points one can conclude that if the second-in-the-pair airplane flies within this zone, the collision with the shell case will occur (Fig.12). The plots proved that increase in the initial velocity of the shell case moved upwards the locations of the shell-case dispertion zones in space (Fig.13).

Fig.13 shows the zone of possible collisions of the shell case with the second-in-the-pair airplane as referred to the above-presented location in space.

Zones of dispersion of shell cases in the atmosphere described with the

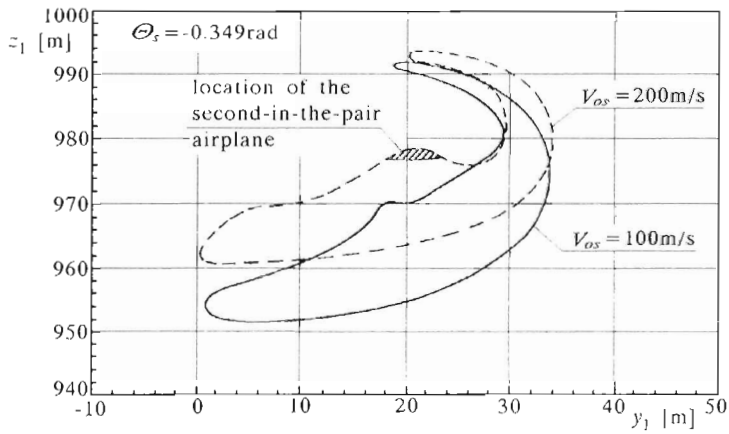

Fig. 13. Comparison between the zones of dispersion of shell cases in space, with the atmosphere at rest assumed

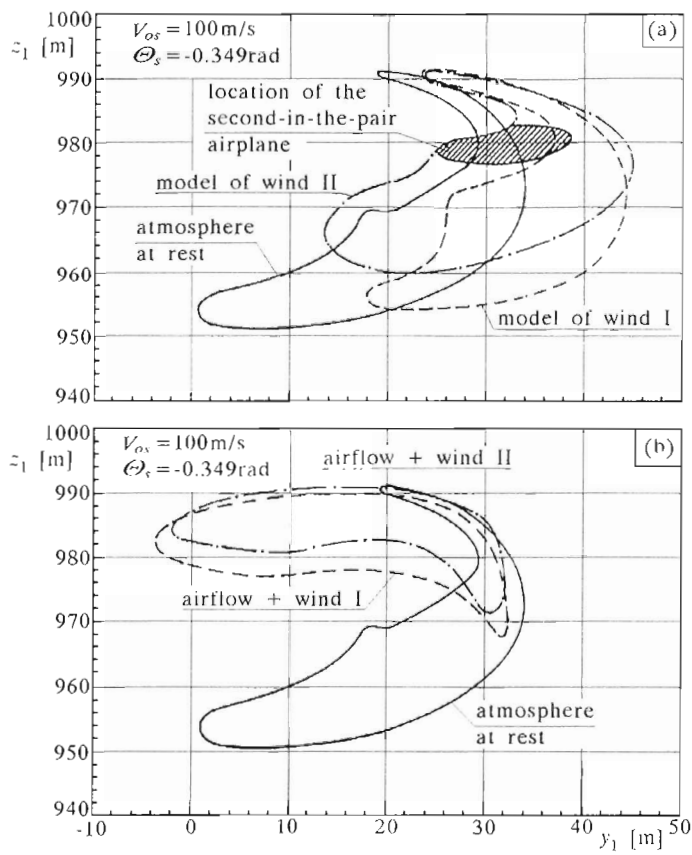

Fig. 14. Comparison between the zones of dispersion of shell cases in the atmosphere at rest and with the air mass motion, i.e. with: (a) models of wind, (b) model of the behind-the-wing airflow + wind taken into account

above-presented models of:

- wind I,
- wind II,
- airflow behind the wing and wind I,
- airflow behind the wing and wind II,

are given below (for the airspeed $V_{os} = 100\,\mathrm{m/s}$).

Fig.14 shows the results of research compared with the solutions obtained for the case of the air mass motion neglected. The comparative study proves a considerable influence of the air parameters (determined using the models mentioned) upon the zones of dispersion of shell cases.

Analysis of both the zones of dispersion of shell cases and the co-ordinates of location of the second-in-the-pair airplane in space shows that:

- In the case of *atmosphere at rest* the second-in-the-pair airplane in the manoeuvre of attack (in some three-dimensional location relative to the lead airplane) is in the zone of shell-case dispersion while flying with the airspeed $V_{os} = 200\,\mathrm{m/s}$ (shaded area in Fig.13)

- In the case of taking influence of the *air mass motion* into account, the zones of dispersion of shell cases (with both models of wind and airflow behind the wing given consideration) are shifted upwards as compared to the zone for which the air mass motion has been neglected. The second-in-the-pair airplane in the manoeuvre of attack (in some three-dimensional location relative to the lead airplane) is to be found in the upper area of the zone (Fig.14).

References

1. ETKIN B., 1972, *Dynamics of Atmospheric Flight*, John Wiley and Sons, Inc., PWN, New York

2. MANEROWSKI J., 1990, Identyfikacja modelu dynamiki lotu odrzutowego samolotu oraz jego układów sterowania, *Prace Naukowe ITWL*, 296

3. MANEROWSKI J., NOWAKOWSKI M., RYMASZEWSKI S., 1990, Komputerowy model dynamiki lotu samolotu zweryfikowany próbami w locie, *MTiS*, **28**, 3-4

4. MARYNIAK J., NOWAKOWSKI M., 1990, Charakterystyki aerodynamiczne luski naboju działka lotniczego w opływie przestrzennym, *MTiS*, **28**, 3-4

5. SUSŁOW G.K., 1960, *Mechanika teoretyczna*, PWN, Warszawa

Modelowanie i analiza dynamiki lotu łuski

Streszczenie

W pracy przedstawiono modele matymatyczny, fizyczny i komputerowy dynamiki lotu łuski. Wymienione modele opracowano w oparciu o wyniki prac z zakresu dynamiki obiektów latających oraz dane uzyskane z badań tunelowych. Do rozwiązania układu równań różniczkowych zwyczajnych opisujących ruch łuski zastosowano metodę numerycznego całkowania równań Rungego-Kutty-Gilla. W oparciu o wyżej wymieniony model.

- przeprowadzono analizę parametrów ruchu łuski działka lotniczego, wyrzucanej z samolotu w dowolnym locie przestrzennym z uwzględnieniem rzeczywistych parametrów atmosfery oraz ruchu mas powietrza (wiatru i strumienia zaskrzydlowego),
- określono strefy rozrzutu łusek w przestrzeni i względem samolotu prowadzonego podczas grupowego atakowania celu.

Manuscript received April 24, 1997; accepted for print July 10, 1997